Journal of Histochemistry & Cytochemistry 2022, Vol. 70(9) 659–667

DOI: 10.1369/00221554221120301
journals.sagepub.com/home/jhc
SAGE

Tuft Cells Are Present in Submandibular Glands Across Species

Harim Tavares dos Santos, Kihoon Nam, Frank M. Maslow, Travis Small, Tabitha L.I. Galloway, Laura M. Dooley, Patrick T. Tassone, Robert P. Zitsch III, Gary A. Weisman, and Olga J. Baker

Department of Otolaryngology-Head and Neck Surgery (HTDS, KN, FMM, TS, TLIG, LMD, PTT, RPZ, OJB), Department of Biochemistry (GAW, OJB), and Christopher S. Bond Life Sciences Center (HTDS, KN, FMM, TS, GAW, OJB), University of Missouri, Columbia, Missouri

Summary

Tuft cells are bottle-shaped, microvilli-projecting chemosensory cells located in the lining of a variety of epithelial tissues and, following their identification approximately 60 years ago, have been linked to immune system function in a variety of epithelia. Until recently, Tuft cells had not been convincingly demonstrated to be present in salivary glands with their detection by transmission electron microscopy only shown in a handful of earlier studies using rat salivary glands, and no follow-up work has been conducted to verify their presence in salivary glands of other species. Here, we demonstrate that Tuft cells are present in the submandibular glands of various species (i.e., mouse, pig and human) using transmission electron microscopy and confocal immunofluorescent analysis for the POU class 2 homeobox 3 (POU2F3), which is considered to be a master regulator of Tuft cell identity. (J Histochem Cytochem 70: 659–667, 2022)

Keywords

chemosensation, immunology, secretion, taste receptors

Introduction

Tuft cells (TC) were identified over 60 years ago by Rhodin & Dalhamn while investigating tracheal epithelial structure using transmission electron microscopy (TEM).[1,2] TC were identified using morphological criteria alone (i.e., the presence of rare bottle-shaped cells with "tuft-like" brush apical microvilli) in multiple tissues including airways, nasopharyngeal cavities, and the intestine,[1,3–6] and they have since been described as cholinergic chemosensory epithelial cells that play a role in signal transduction across epithelia.[7,8] Moreover, TC have been shown to regulate innate immune responses to various microbial stimuli,[9–11] to help modulate tissue repair,[12,13] and host-defense responses.[14,15] While these studies provide some understanding of TC features and function, these cells remain understudied in all organs, particularly salivary glands where they have only been identified by a single research group in excretory ducts of rat salivary glands.[16] Thus, the current paper seeks to identify TC in salivary glands from several species (i.e., mouse, pig, and human) to more widely establish their presence in the salivary glands. For this purpose, we employed transmission electron microscopy and confocal immunofluorescent analysis for POU class 2 homeobox 3 (POU2F3), which is considered to be a master regulator of TC identity because knocking out its gene leads to a complete lack of TC.[11,17–21] This combination of ultrastructural analysis and confocal microscopy provides the gold standard for unambiguous identification of TC,[22,23] whereas previous studies have shown poor recognition of this rare cell type by the more commonly chosen method of hematoxylin and eosin (H&E) staining.[24]

Received for publication June 9, 2022; accepted July 27, 2022.

Corresponding Author:
Olga J. Baker, Department of Otolaryngology-Head and Neck Surgery, Department of Biochemistry, School of Medicine, University of Missouri, 540B Christopher S. Bond Life Sciences Center, 1201 Rollins Street, Columbia, MO 65211-7310, USA.
E-mail: bakero@health.missouri.edu

Journal of Histochemistry & Cytochemistry

Materials and Methods

Materials

Rabbit anti-mouse/human POU class 2 homeobox 3 (POU2F3) antibody (e.g., to detect this protein in mouse and human tissues) was obtained from Mybiosource (Vancouver, Canada). Rabbit anti-pig POU2F3 antibody (e.g., to detect this protein in pig tissue) was obtained from Sigma (St. Louis, MO). Mouse anti-mouse/pig/human cytokeratin-7 antibody (ductal marker) was obtained from Abcam (Cambridge, MA). Alexa Fluor 488-conjugated anti-rabbit IgG, Alexa Fluor 568-conjugated anti-mouse IgG, phosphate buffered saline (PBS), 4′,6-diamidino-2-phenylindole (DAPI), triton X-100, sodium citrate, xylene and ethanol were purchased from Thermo Fisher Scientific (Waltham, MA).

Animals

Three female C57BL/6J mice from Jackson Laboratory at 5-6 weeks of age were euthanized with CO_2 (30% per minute) followed by abdominal exsanguination and removal of the submandibular glands (SMG). All animal management and procedures were approved by the Animal Care and Use Committee of the University of Missouri. Submandibular glands from two female pigs at 3 years of age were purchased from Zyagen (San Diego, CA) and processed, as detailed below. Finally, small intestine sections from all species herein evaluated were purchased from Zyagen for use as a positive control.

Human Subjects

Three human SMG from female subjects (average age: 76.3 years old) were obtained from the University of Missouri, Department of Otolaryngology, Head and Neck Surgery. Note that tissues are healthy submandibular gland tissue from head and neck cancer patients undergoing neck dissections that would otherwise be discarded. Usage of all human specimens was conducted under the guidelines and with the approval of the University of Missouri Health Sciences Institutional Review Board and informed consent was obtained for each patient.

Transmission Electron Microscopy

Mouse, pig, and human SMG were fixed using 2% (v/v) glutaraldehyde and 2% (v/v) formaldehyde (prepared from paraformaldehyde) in 0.1 M cacodylate buffer, pH 7.2, overnight at 4°C. Fixed specimens were then rinsed four times for 10 min each with 30 mM HEPES, pH 7.2, 70 mM NaCl, and 6% (w/v) sucrose, rinsed three times with 20 mM Tris, pH 7.2, containing 120 mM NaCl and 5 mM $CaCl_2$, postfixed with osmium tetroxide 1% (w/v) OsO_4, 70 mM NaCl, 5 mM $CaCl_2$, 30 mM HEPES buffer, pH 7.4, for 10 min, and rinsed three times for 10 min each with distilled water. Fixed samples were stained overnight in aqueous 0.5% (w/v) uranyl acetate, pH 6.0, at room temperature and infiltrated with Epon-Araldite epoxy resin (Electron Microscopy Sciences, Hatfield, PA). The infiltrate was placed in fresh resin in ballistic electron-emission microscopy (BEEM) embedding capsules and polymerized at 60°C. Sections of 70 nm thickness were cut on a Leica ultra-cut microtome (UCT) and stained with 5% (w/v) uranyl acetate and Sato's triple lead salt stain consisting of 1% (w/v) lead citrate, 1% (w/v) lead acetate, 1% (w/v) lead nitrate, and 2% (w/v) sodium citrate. Samples were viewed and photographed with a Japan Electro Optics Laboratories (JEOL 1400) transmission electron microscope.

Immunofluorescence

Mouse, pig, and human SMG were fixed in 10% (v/v) formalin for 24 hr at room temperature and later transferred to 70% (v/v) ethanol. Next, SMG were dehydrated through a series of graded ethanol baths, embedded in paraffin, and cut into 5 µm sections. SMG paraffin-embedded slides from all species (i.e., mouse, pig, and human) were then deparaffinized by washing three times for 5 min in 100% xylene. Slides were then washed for 5 min in xylene: ethanol (1:1), twice for 5 min in 100% ethanol, followed by 5 min washes once each in 95%, 80%, 70%, and 50% (v/v) ethanol and twice in distilled water. Then, deparaffinized tissue sections were incubated with sodium citrate buffer, 10 mM sodium citrate, 0.05% (v/v) Tween 20, pH 6.0, at 95°C for 30 min for antigen retrieval. Next, samples were rinsed twice with distilled water and permeabilized with 0.1% (v/v) Triton X-100 in PBS at room temperature for 45 min. Sections were then blocked with 5% (v/v) goat serum in PBS at room temperature for 1 hr and incubated with rabbit anti-POU2F3 antibody (1:500) for mouse and human SMG and (1:500) for pig SMG as well as mouse-anti-cytokeratin-7 (1:100, ductal marker) for all samples at 4°C overnight. Then, specimens were washed three times with PBS and incubated with Alexa Fluor 488-conjugated anti-rabbit IgG (1:500; A-11008, ThermoFisher) at room temperature for 1 hr. Finally, sections were washed three times with PBS and counterstained with DAPI iodide at room temperature for 15 min (1:1,000 dilution) and images were captured with a 63× objective and analyzed using a confocal Stellaris 5 Leica microscope. Finally, positive controls from all species were processed as detailed above and are shown in Supplemental Fig. 1.

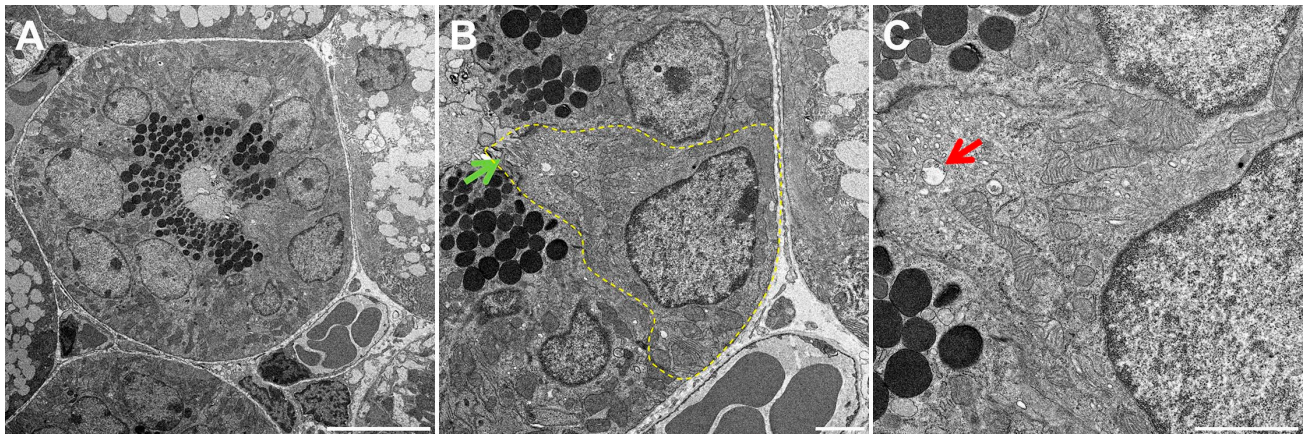

Figure 1. Fine structure of Tuft cells (TC) of mouse SMG. Shown is a transmission electron micrograph of TC in a mouse SMG striated duct (A). Note the bottle-like cell shape at the nucleus with narrow apical and basal portions consistent with TC morphology (B). There are numerous apical vesicles in the supranuclear cytoplasm (C). The yellow dotted line indicates a TC while the green and red arrows denote characteristic apical microvilli and tubulovesicular system, respectively. Scale bars represent 10 (A), 2 (B), and 2 (C) µm, respectively. Abbreviations: SMG, submandibular glands.

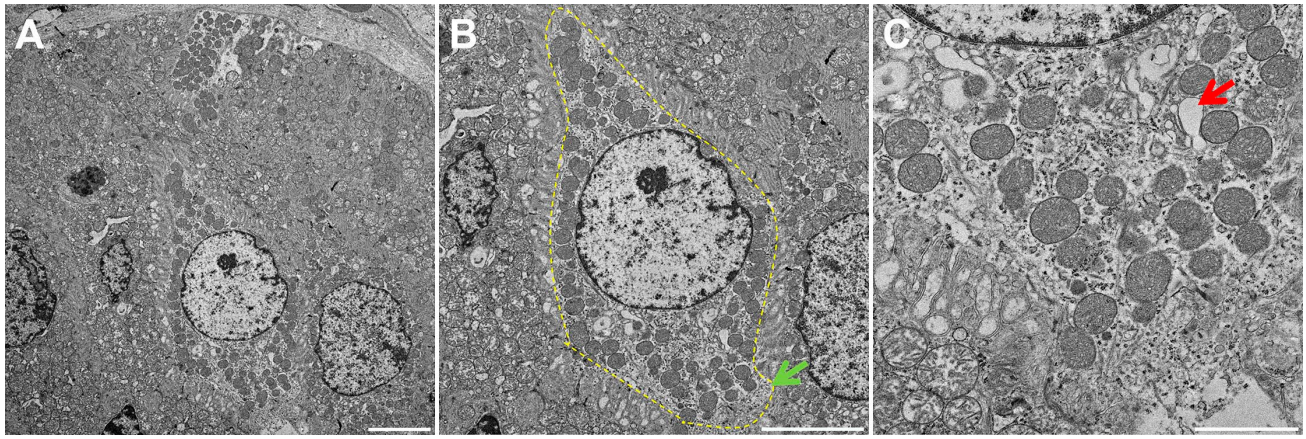

Figure 2. Fine structure of Tuft cells (TC) of pig SMG. Shown is a transmission electron micrograph of TC in a pig SMG striated duct (A). Note the bottle-like cell shape at the nucleus with narrow apical and basal portions consistent with TC morphology (B). There are numerous apical vesicles in the supranuclear cytoplasm (C). The yellow dotted line indicates a TC while the green and red arrows denote apical microvilli and the tubulovesicular system. Scale bars represent 5 (A), 5 (B) and 2 (C) µm, respectively. Abbreviations: SMG, submandibular glands; TC, Tuft cells.

Results

Identification of Tuft Cells in Submandibular Glands Using Ultrastructural Analysis

Using TEM, we were able to identify structures consistent with TC in mouse, pig and human SMG. In mice, we observed bottle-shaped cells lacking secretory granules with a distinct cluster of microvilli at the narrow apical surface (Fig. 1A and B, yellow dotted area). Notably, the apical microvilli were thicker and longer than those observed in neighboring cells (Fig. 1B, green arrow), consistent with the presence of TC in mouse SMG epithelia. Moreover, multiple apical vesicles were observed in the supranuclear cytoplasm (Fig. 1C, red arrow), while TC were likewise noted to be present in the striated ducts of mouse SMG but absent in other related structures (i.e., in the acinus, intercalated duct and excretory duct). As for pig and human tissues (Figs. 2A and B and 3A and B, yellow dotted areas), we observed similar TC features as in mouse SMG, except that the apical microvilli surface was less developed (i.e., shorter) (Figs. 2B and 3B, green arrows). Finally, multiple apical vesicles were detected in the supranuclear cytoplasm from pigs and human tissues (Figs. 2C and 3C, red arrows). Together, these results indicate that mouse, pig and human SMG display a cell type consistent with TC in striated ducts with remarkable similarity across these species.

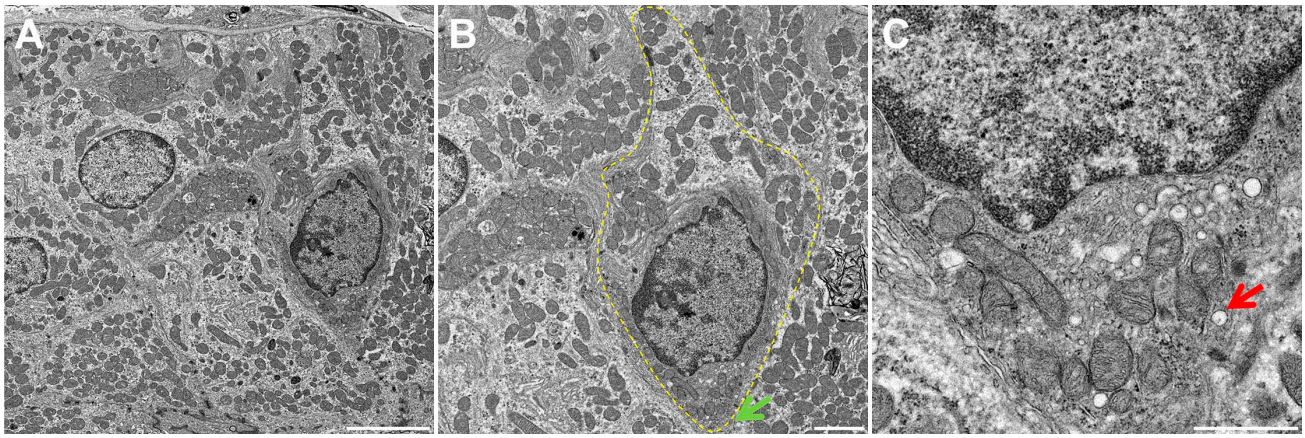

Figure 3. Fine structure of Tuft cells (TC) of human SMG. Shown is a transmission electron micrograph of TC in a human SMG striated duct (A). Note the bottle-like cell shape at the nucleus with narrow apical and basal portions consistent with TC morphology (B). There are numerous apical vesicles in the supranuclear cytoplasm (C). The yellow dotted line indicates a TC while the green and red arrows denote characteristic apical microvilli and the tubulovesicular system. Scale bars represent 5 (A), 2 (B), and 1 (C) μm, respectively. Abbreviations: SMG, submandibular glands; TC, Tuft cells.

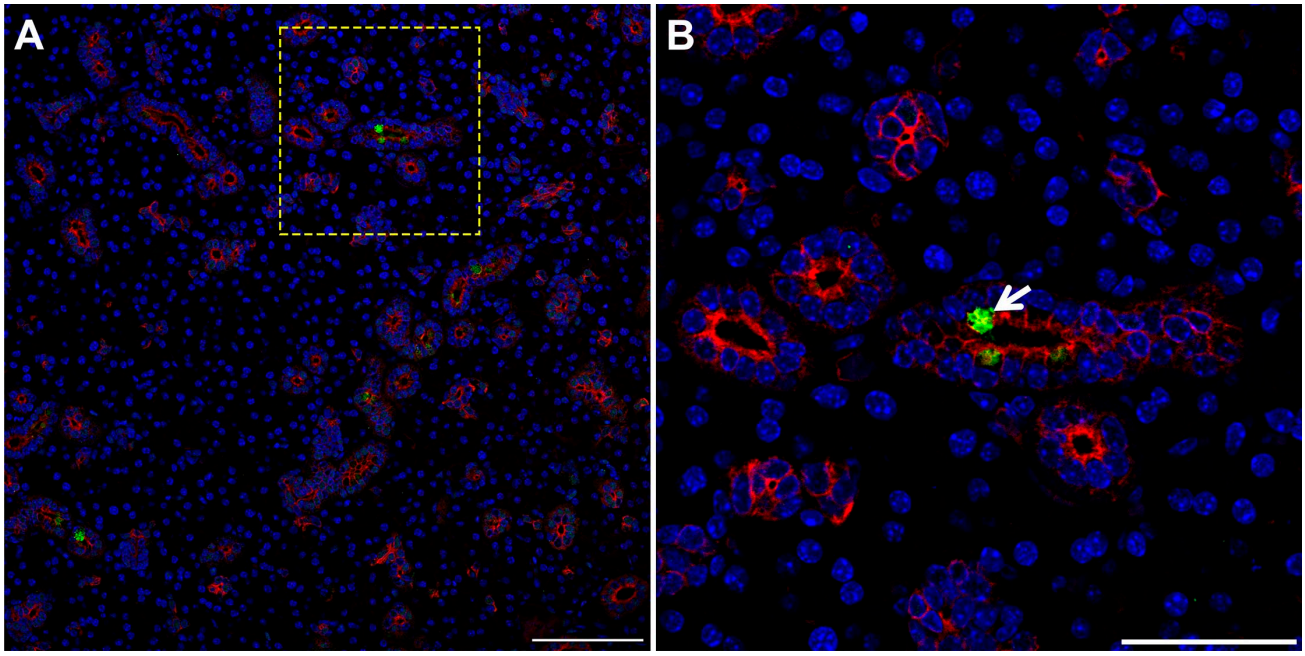

Figure 4. TC are present in mouse SMG. Five microns of a paraffin embedded SMG section were stained with rabbit anti-POU2F3 and mouse anti-cytokeratin-7, followed by anti-rabbit Alexa Fluor 488 (green) and anti-mouse Alexa Fluor 568 IgG (red) secondary antibodies and counterstained with 4,'6-diamidino-2-phenylindole (blue). Images were analyzed using a Stellaris microscope at low (A) and high (B) magnifications. Yellow dotted lines indicate area that was magnified. White arrow denotes TC in SMG duct. Images are representative of n = 3 specimens. Scale bars from low and high magnification represent 100 and 50 μm, respectively. Abbreviations: SMG, submandibular glands; TC, Tuft cells.

Identification of Tuft Cells in Submandibular Glands Using Confocal Analysis

While the results above showed cells consistent with TC morphology within mouse, pig and human SMG, we confirmed their identity using a specific TC marker. Our results indicate that striated ducts of mouse (Fig. 4, white arrow), pig (Fig. 5, white arrow), and human (Fig. 6, white arrow) SMG display positive staining for POU class 2 homeobox 3 (POU2F3, herein employed as a master regulator of TC identity as detailed above).[11,17–21] Together, these results indicate for the first time the presence of TC in striated ducts of SMG in mice, pigs and humans.

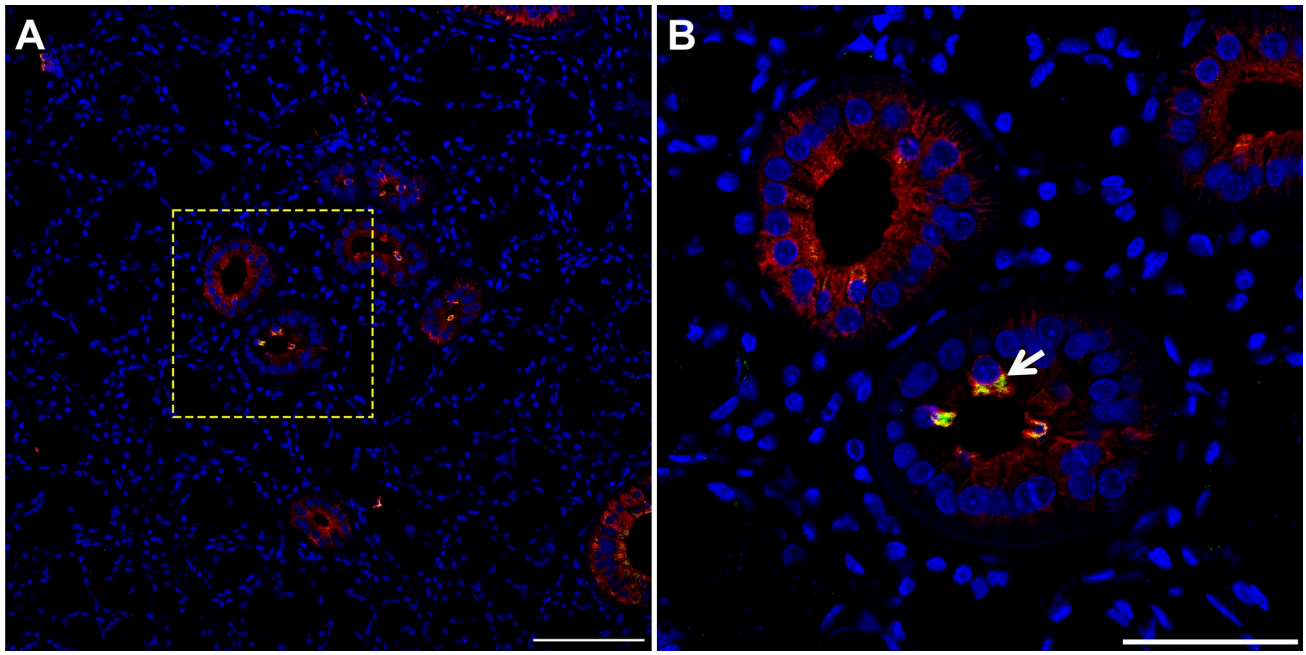

Figure 5. TC are present in pig SMG. Five microns of a paraffin embedded SMG section were stained with rabbit anti-POU2F3 and mouse anti-cytokeratin-7, followed by anti-rabbit Alexa Fluor 488 (green) and anti-mouse Alexa Fluor 568 immunoglobulin G (red) secondary antibodies and counterstained with 4',6-diamidino-2-phenylindole (blue). Images were analyzed using a Stellaris microscope at low (A) and high (B) magnifications. Yellow dotted lines indicate area that was magnified. White arrow denotes TC in SMG duct. Scale bars from low and high magnification represent 100 and 50 μm, respectively. Abbreviations: SMG, submandibular glands; TC, Tuft cells.

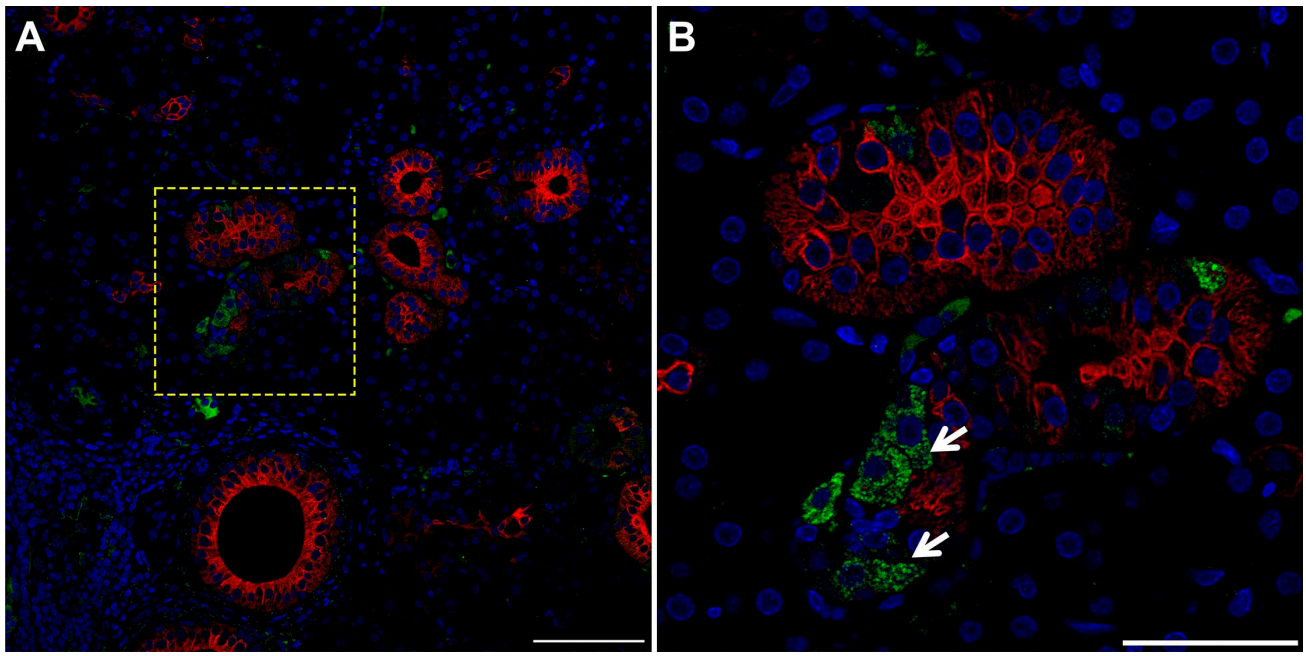

Figure 6. TC are present in human SMG. Five microns of a paraffin embedded SMG section were stained with rabbit anti-POU2F3 and mouse anti-cytokeratin-7, followed by anti-rabbit Alexa Fluor 488 (green) and anti-mouse Alexa Fluor 568 immunoglobulin G (red) secondary antibodies and counterstained with 4',6-diamidino-2-phenylindole (blue). Images were analyzed using a Stellaris microscope at low (A) and high (B) magnifications. Yellow dotted lines indicate area that was magnified. White arrow denotes TC in SMG duct. Images are representative of n = 3 specimens. Scale bars from low and high magnification represent 100 and 50 μm, respectively. Abbreviations: SMG, submandibular glands; TC, Tuft cells.

Discussion

We demonstrated the presence of TC in striated ducts of mouse, pig, and human SMG. To the best of our knowledge, this is the first study showing TC in salivary glands of these species and encourages further investigation of TC function in salivary glands. In other epithelia, TC have been shown to regulate immunomodulatory pathways via chemosensory signaling. Studies have shown that TC express taste receptor (TasR) signaling genes, including α-gustducin,[25] transient receptor potential cation channel subfamily M member 5 (*Trpm5*),[26,27] and phospholipase Cβ2 (Plcβ2).[28] Moreover, TC modulate the expression of neuronal and inflammatory gene pathways (e.g., enzymes and are involved in the biosynthesis of acetylcholine [Ach][29] and eicosanoids[30,31] as well as interleukin ([IL]-25).[9–11] Other studies in epithelial tissues have demonstrated that TC respond to stimuli via activation of taste receptors and their downstream signaling molecules, leading to the release of effector proteins that activate neighboring epithelial cells and sub-epithelial immune and non-immune cells.[32–34] Additionally, TC have been shown to be the primary source of IL-25 in the intestine whose release increases in response to parasites.[9–11] Specifically, IL-25 stimulates innate lymphoid cells to release IL-13, which provokes epithelial remodeling as evidenced by expansion of TC and goblet cells that ultimately leads to parasite removal through the increased production of mucus.[9–11] Additionally, deletion of *Pou2f3* results in complete ablation of intestinal TC and defective immune responses to parasites,[11] while airways of *Pou2f3* knockout mice likewise display and absence of TC[17,18] together with decreased leukotrienes and IL-25 secretion.[35,36] Despite the clear evidence of TC contribution to immune functioning presented above, the functional role of TC remains poorly understood in salivary glands. To begin filling this gap in the oral health literature, we postulate that activation of chemosensory receptors in TC regulate both innate and adaptive immune responses within the salivary gland as occurs in other epithelial tissues.[28,37] Based on our findings of the existence of TC within striated salivary glands of mouse, pigs, and humans, future studies are needed to determine whether the primary role of TC is to regulate chemosensory and immunomodulatory pathways in these salivary glands.

Regarding specific secretory functions, previous studies have shown that TC produce and secrete Ach.[15,38,39] Since Ach release in airway epithelia promotes antimicrobial peptide secretion,[14,40] we postulate that TC in salivary glands release Ach to regulate the antimicrobial peptide (e.g., defensins, cathelicidins, and histatins) composition of saliva.[41,42] Considering it is well-established that salivary gland fluid secretion is mediated by activation of muscarinic receptors via the release of neuronal Ach,[43–45] it is possible that TC in salivary glands also promote Ach-mediated saliva secretion from salivary acinar epithelial cells, which would represent a novel TC function. Therefore, future studies should assess the role of TC in the regulation of saliva quantity and quality that could be relevant to the treatment of salivary gland hypofunction as seen in the autoimmune disease Sjögren's syndrome[46] and radiation-induced damage of salivary glands caused by radiotherapy for head and neck cancers.[47]

In summary, this study demonstrates for the first time that TC are present in the striated ducts of salivary glands of mouse, pigs, and humans (Fig. 7), which incentivizes future investigation on the role of salivary TC in oral health and disease. Based on these and previous findings, we postulate that salivary TC play a role in the regulation of saliva secretion and innate and adaptive immunity, which warrants further elucidation.

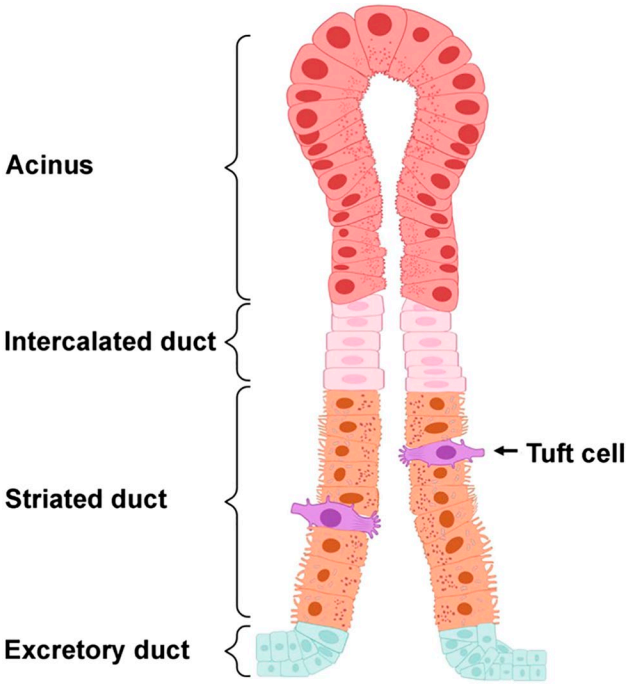

Figure 7. Diagram representing the localization of Tufts cells in salivary glands based on the findings obtained in this study. Salivary gland structure consists of secretory acini and ducts (i.e., intercalated, striated and excretory). In this diagram, Tuft cells were depicted by their distinct bottle-shaped morphology and well-developed "tuft-like" microvilli at the apical surface. As for their location, these cells were restricted to striated ductal epithelia. Created using Biorender.com.

Competing Interests

The author(s) declared no potential conflicts of interest with respect to the research, authorship, and/or publication of this article.

Author Contributions

HTS and OB, conceived and designed the study; HTS, performed the experiments; HTS, KN, FM, TS, TG, LD, PT, RZ, GW and OB, contributed to data analysis; HTS and OB, drafted the manuscript. All authors read and approved the final manuscript.

Funding

The author(s) disclosed receipt of the following financial support for the research, authorship, and/or publication of this article: This study was supported by the National Institutes of Health-National Institute of Dental and Craniofacial Research Grants (R01DE022971 and R01DE027884 to OJB and R01DE007389 and R01DE029833 to GAW).

ORCID iDs

Kihoon Nam https://orcid.org/0000-0001-8934-4886
Patrick T. Tassone https://orcid.org/0000-0001-8633-2126
Olga J. Baker https://orcid.org/0000-0002-0628-8645

Supplemental Material

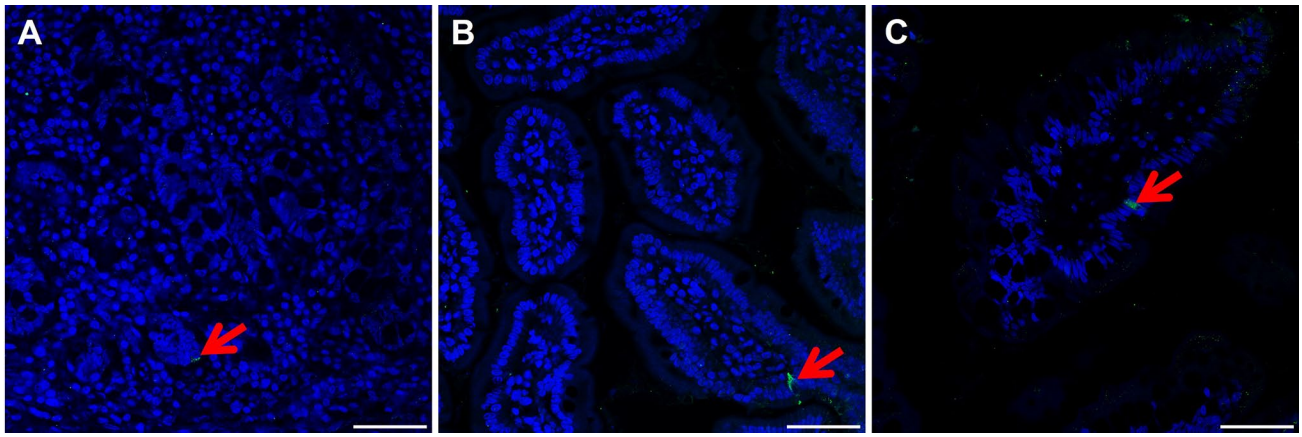

Supplemental Figure 1. Positive controls for the POU2F3 antibody. Five microns of a paraffin embedded small intestine sections from mouse (A), pig (B) and humans (C) were stained with rabbit anti-POU2F3 followed by anti-rabbit Alexa Fluor 488 (green) and counterstained with DAPI (blue). Images were analyzed using a Stellaris microscope at 40 magnification. White arrow denotes TC in small intestine epithelium. Scale bars = 50 μm.

Literature Cited

1. Rhodin J, Dalhamn T. Electron microscopy of the tracheal ciliated mucosa in rat. Z Zellforsch Mikrosk Anat. 1956;44(4):345–412.
2. Sato A, Miyoshi S. Fine structure of tuft cells of the main excretory duct epithelium in the rat submandibular gland. Anat Rec. 1997;248(3):325–31.
3. Finger TE, Böttger B, Hansen A, Anderson KT, Alimohammadi H, Silver WL. Solitary chemoreceptor cells in the nasal cavity serve as sentinels of respiration. Proc Natl Acad Sci U S A. 2003;100(15):8981–6.
4. Jarvi O, Keyrilainen O. On the cellular structures of the epithelial invasions in the glandular stomach of mice caused by intramural application of 20-methylcholantren. Acta Pathol Microbiol Scand Suppl. 1956;39(Suppl 111):72–3.
5. Luciano L, Castellucci M, Reale E. The brush cells of the common bile duct of the rat. This section, freeze-fracture and scanning electron microscopy. Cell Tissue Res. 1981;218(2):403–20.
6. Panneck AR, Rafiq A, Schütz B, Soultanova A, Deckmann K, Chubanov V, Gudermann T, Weihe E, Krasteva-Christ G, Grau V, del Rey A, Kummer W. Cholinergic epithelial cell with chemosensory traits in murine thymic medulla. Cell and Tissue Research. 2014;358(3):737–48.
7. Sbarbati A, Bramanti P, Benati D, Merigo F. The diffuse chemosensory system: exploring the iceberg toward the definition of functional roles. Prog Neurobiol. 2010;91(1):77–89.
8. Kusumakshi S, Voigt A, Hübner S, Hermans-Borgmeyer I, Ortalli A, Pyrski M, Dörr J, Zufall F, Flockerzi V, Meyerhof W, Montmayeur JP, Boehm U. A binary genetic approach to characterize TRPM5 cells in mice. Chem Senses. 2015;40(6):413–25.
9. von Moltke J, Ji M, Liang H-E, Locksley RM. Tuft-cell-derived IL-25 regulates an intestinal ILC2–epithelial response circuit. Nature. 2016;529(7585):221–5.
10. Howitt MR, Lavoie S, Michaud M, Blum AM, Tran SV, Weinstock JV, Gallini CA, Redding K, Margolskee RF, Osborne LC, Artis D, Garrett WS. Tuft cells, taste-chemosensory cells, orchestrate parasite type 2 immunity in the gut. Science. 2016;351(6279):1329–33.
11. Gerbe F, Sidot E, Smyth DJ, Ohmoto M, Matsumoto I, Dardalhon V, Cesses P, Garnier L, Pouzolles M, Brulin B, Bruschi M, Harcus Y, Zimmermann VS, Taylor N, Maizels RM, Jay P. Intestinal epithelial tuft cells initiate type 2 mucosal immunity to helminth parasites. Nature. 2016;529(7585):226–30.

12. Chandrakesan P, May R, Weygant N, Qu D, Berry WL, Sureban SM, Ali N, Rao C, Huycke M, Bronze MS, Houchen CW. Intestinal tuft cells regulate the ATM mediated DNA Damage response via Dclk1 dependent mechanism for crypt restitution following radiation injury. Sci Rep. 2016;6:37667.
13. May R, Qu D, Weygant N, Chandrakesan P, Ali N, Lightfoot SA, Li L, Sureban SM, Houchen CW. Brief report: Dclk1 deletion in tuft cells results in impaired epithelial repair after radiation injury. Stem Cells. 2014;32(3):822–7.
14. Tizzano M, Gulbransen BD, Vandenbeuch A, Clapp TR, Herman JP, Sibhatu HM, Churchill ME, Silver WL, Kinnamon SC, Finger TE. Nasal chemosensory cells use bitter taste signaling to detect irritants and bacterial signals. Proc Natl Acad Sci U S A. 2010;107(7):3210–5.
15. Krasteva G, Canning BJ, Hartmann P, Veres TZ, Papadakis T, Mühlfeld C, Schliecker K, Tallini YN, Braun A, Hackstein H, Baal N, Weihe E, Schütz B, Kotlikoff M, Ibanez-Tallon I, Kummer W. Cholinergic chemosensory cells in the trachea regulate breathing. Proc Natl Acad Sci U S A. 2011;108(23):9478–83.
16. Sato A. Scanning and transmission electron microscopical study of the main excretory duct of the rat major salivary glands. J Kyushu Dent Soc. 1982;36:610–31.
17. Ohmoto M, Yamaguchi T, Yamashita J, Bachmanov AA, Hirota J, Matsumoto I. Pou2f3/Skn-1a is necessary for the generation or differentiation of solitary chemosensory cells in the anterior nasal cavity. Biosci Biotechnol Biochem. 2013;77(10):2154–6.
18. Yamashita J, Ohmoto M, Yamaguchi T, Matsumoto I, Hirota J. Skn-1a/Pou2f3 functions as a master regulator to generate Trpm5-expressing chemosensory cells in mice. PLoS ONE. 2017;12(12):e0189340.
19. Yamaguchi T, Yamashita J, Ohmoto M, Aoudé I, Ogura T, Luo W, Bachmanov AA, Lin W, Matsumoto I, Hirota J. Skn-1a/Pou2f3 is required for the generation of Trpm5-expressing microvillous cells in the mouse main olfactory epithelium. BMC Neurosci. 2014;15:13.
20. Matsumoto I, Ohmoto M, Narukawa M, Yoshihara Y, Abe K. Skn-1a (Pou2f3) specifies taste receptor cell lineage. Nat Neurosci. 2011;14(6):685–7.
21. Huang Y-H, Klingbeil O, He X-Y, Wu XS, Arun G, Lu B, Somerville TDD, Milazzo JP, Wilkinson JE, Demerdash OE, Spector DL, Egeblad M, Shi J, Vakoc CR. POU2F3 is a master regulator of a tuft cell-like variant of small cell lung cancer. Genes Dev. 2018;32(13-14):915–28.
22. DelGiorno KE, Naeem RF, Fang L, Chung CY, Ramos C, Luhtala N, O'Connor C, Hunter T, Manor U, Wahl GM. Tuft cell formation reflects epithelial plasticity in pancreatic injury: implications for modeling human pancreatitis. Front Physiol. 2020;11:88.
23. Bohórquez D, Haque F, Medicetty S, Liddle RA. Correlative confocal and 3D electron microscopy of a specific sensory cell. J Vis Exp. 2015;101:e52918.
24. Esmaeilniakooshkghazi A, George SP, Biswas R, Khurana S. Mouse intestinal tuft cells express advillin but not villin. Sci Rep. 2020;10(1):8877.
25. Höfer D, Püschel B, Drenckhahn D. Taste receptor-like cells in the rat gut identified by expression of alpha-gustducin. Proc Natl Acad Sci U S A. 1996;93(13):6631–4.
26. Bezençon C, le Coutre J, Damak S. Taste-signaling proteins are coexpressed in solitary intestinal epithelial cells. Chem Senses. 2007;32(1):41–9.
27. Iwatsuki K, Torii K. Peripheral chemosensing system for tastants and nutrients. Curr Opin Endocrinol Diabetes Obes. 2012;19(1):19–25.
28. Nadjsombati MS, McGinty JW, Lyons-Cohen MR, Jaffe JB, DiPeso L, Schneider C, Miller CN, Pollack JL, Nagana Gowda GA, Fontana MF, Erle DJ, Anderson MS, Locksley RM, Raftery D, von Moltke J. Detection of succinate by intestinal tuft cells triggers a type 2 innate immune circuit. Immunity. 2018;49(1):33–41.e7.
29. Schütz B, Ruppert AL, Strobel O, Lazarus M, Urade Y, Büchler MW, Weihe E. Distribution pattern and molecular signature of cholinergic tuft cells in human gastro-intestinal and pancreatic-biliary tract. Sci Rep. 2019;9(1):17466.
30. Bezençon C, Fürholz A, Raymond F, Mansourian R, Métairon S, Le Coutre J, Damak S. Murine intestinal cells expressing Trpm5 are mostly brush cells and express markers of neuronal and inflammatory cells. J Comp Neurol. 2008;509(5):514–25.
31. Haber AL, Biton M, Rogel N, Herbst RH, Shekhar K, Smillie C, Burgin G, Delorey TM, Howitt MR, Katz Y, Tirosh I, Beyaz S, Dionne D, Zhang M, Raychowdhury R, Garrett WS, Rozenblatt-Rosen O, Shi HN, Yilmaz O, Xavier RJ, Regev A. A single-cell survey of the small intestinal epithelium. Nature. 2017;551(7680):333–9.
32. Ualiyeva S, Lemire E, Aviles EC, Wong C, Boyd AA, Lai J, Liu T, Matsumoto I, Barrett NA, Boyce JA, Haber AL, Bankova LG. Tuft cell-produced cysteinyl leukotrienes and IL-25 synergistically initiate lung type 2 inflammation. Sci Immunol. 2021;6(66):eabj0474.
33. Schumacher MA, Hsieh JJ, Liu CY, Appel KL, Waddell A, Almohazey D, Katada K, Bernard JK, Bucar EB, Gadeock S, Maselli KM, Washington MK, Grikscheit TC, Warburton D, Rosen MJ, Frey MR. Sprouty2 limits intestinal tuft and goblet cell numbers through GSK3β-mediated restriction of epithelial IL-33. Nat Commun. 2021;12(1):836.
34. O'Leary CE, Schneider C, Locksley RM. Tuft cells-systemically dispersed sensory epithelia integrating immune and neural circuitry. Annu Rev Immunol. 2019;37:47–72.
35. Bankova LG, Dwyer DF, Yoshimoto E, Ualiyeva S, McGinty JW, Raff H, von Moltke J, Kanaoka Y, Frank Austen K, Barrett NA. The cysteinyl leukotriene 3 receptor regulates expansion of IL-25-producing airway brush cells leading to type 2 inflammation. Sci Immunol. 2018;3(28):eaat9453.
36. Ualiyeva S, Hallen N, Kanaoka Y, Ledderose C, Matsumoto I, Junger WG, Barrett NA, Bankova LG. Airway brush cells generate cysteinyl leukotrienes through the ATP sensor P2Y2. Sci Immunol. 2020;5(43):eaax7224.
37. Schneider C. Tuft cell integration of luminal states and interaction modules in tissues. Pflügers Arch. 2021;473(11):1713–22.

38. Perniss A, Schmidt P, Soultanova A, Papadakis T, Dahlke K, Voigt A, Schütz B, Kummer W, Deckmann K. Development of epithelial cholinergic chemosensory cells of the urethra and trachea of mice. Cell Tissue Res. 2021;385(1):21–35.
39. Krasteva G, Hartmann P, Papadakis T, Bodenbenner M, Wessels L, Weihe E, Schütz B, Langheinrich AC, Chubanov V, Gudermann T, Ibanez-Tallon I, Kummer W. Cholinergic chemosensory cells in the auditory tube. Histochem Cell Biol. 2012;137(4):483–97.
40. Lee RJ, Kofonow JM, Rosen PL, Siebert AP, Chen B, Doghramji L, Xiong G, Adappa ND, Palmer JN, Kennedy DW, Kreindler JL, Margolskee RF, Cohen NA. Bitter and sweet taste receptors regulate human upper respiratory innate immunity. J Clin Invest. 2014;124(3):1393–405.
41. Tao R, Jurevic RJ, Coulton KK, Tsutsui MT, Roberts MC, Kimball JR, Wells N, Berndt J, Dale BA. Salivary antimicrobial peptide expression and dental caries experience in children. Antimicrob Agents Chemother. 2005;49(9):3883–8.
42. Jurczak A, Kościelniak D, Papież M, Vyhouskaya P, Krzyściak W. A study on β-defensin-2 and histatin-5 as a diagnostic marker of early childhood caries progression. Biol Res. 2015;48(1):61.
43. Nakamura T, Matsui M, Uchida K, Futatsugi A, Kusakawa S, Matsumoto N, Nakamura K, Manabe T, Taketo MM, Mikoshiba K. M(3) muscarinic acetylcholine receptor plays a critical role in parasympathetic control of salivation in mice. J Physiol. 2004;558(Pt 2):561–75.
44. Proctor GB. Muscarinic receptors and salivary secretion. J Appl Physiol. 2006;100(4):1103–4.
45. Proctor GB, Carpenter GH. Regulation of salivary gland function by autonomic nerves. Auton Neurosci. 2007;133(1):3–18.
46. Ngo DYJ, Thomson WM. An update on the lived experience of dry mouth in Sjögren's syndrome patients. Front Oral Health. 2021;2:767568.
47. Jasmer KJ, Gilman KE, Muñoz Forti K, Weisman GA, Limesand KH. Radiation-induced salivary gland dysfunction: mechanisms, therapeutics and future directions. J Clin Med. 2020;9(12):4095.